



HHS Public Access

Author manuscript

Biochem Biophys Res Commun. Author manuscript; available in PMC 2021 February 12.

Published in final edited form as:

Biochem Biophys Res Commun. 2020 February 12; 522(3): 553–559. doi:10.1016/j.bbrc.2019.11.025.

***PRRT2* frameshift mutation reduces its mRNA stability resulting loss of function in Paroxysmal Kinesigenic Dyskinesia**

Yongcheng Pan^{a,b,1}, Qiong Liu^{a,b,1}, Jennifer Zhang^b, Yang Yang^c, Yun Tian^{d,e}, Junsheng Zeng^c, Peng Yin^f, Lin Mei^e, Wen-cheng Xiong^e, Xiao-Jiang Li^{f,*}, Shihua Li^{f,*}, Beisha Tang^{a,c,g,h,*}

^a Key Laboratory of Hunan Province in Neurodegenerative Disorders, Xiangya Hospital, Central South University, Changsha, Hunan, China

^b Department of Human Genetics, Emory University School of Medicine, Atlanta, GA 30322, USA.

^c Department of Neurology, Xiangya Hospital, Central South University, Changsha, Hunan, China

^d Department of Geriatrics, Xiangya Hospital, Central South University, Changsha, Hunan, China.

^e Department of Neurosciences, Case Western Reserve University, Cleveland, OH 44106, USA

^f Guangdong-Hongkong-Macau Institute of CNS Regeneration, Ministry of Education CNS Regeneration Collaborative Joint Laboratory, Jinan University, Guangzhou, China

^g National Clinical Research Center for Geriatric Disorders, Xiangya Hospital, Central South University, Changsha, Hunan, China

^h Center for Medical Genetics, School of Life Sciences, Central South University, Changsha, Hunan, China

Abstract

A heterozygous frameshift *PRRT2* mutation (c.649_650InsC) has been identified as the major causative mutation in several paroxysmal disorders, including paroxysmal kinesigenic dyskinesia (PKD). Since PKD is an autosomal dominant disorder and since the frameshift mutations of *PRRT2* may create a truncated protein, it remains unclear whether this mutation causes toxic gain of function or loss of function. By generating *PRRT2* knock-in (KI) mice that express human *PRRT2* with the c.649_650InsC mutation and by comparing the phenotypes of *PRRT2* KI mice with *Prrt2* knockout (KO) mice, we find that both KI and KO mice show the same extents of

*Corresponding author: Beisha Tang, Department of Neurology, Xiangya Hospital, 87 of Xiangya Road, Changsha, Hunan Province, China; National Clinical Research Center for Geriatric Medicine, Changsha, Hunan, China; Key Laboratory of Hunan Province in Neurodegenerative Disorders, Central South University, Changsha, Hunan, China; Center for Medical Genetics, School of Life Sciences, Central South University, Changsha, Hunan, China, bstang7398@163.com; Shihua Li, Guangdong-Hongkong-Macau Institute of CNS Regeneration, Ministry of Education CNS Regeneration Collaborative Joint Laboratory, Jinan University, Guangzhou, China, lishihualis@jnu.edu.cn; Xiao-Jiang Li, Guangdong-Hongkong-Macau Institute of CNS Regeneration, Ministry of Education CNS Regeneration Collaborative Joint Laboratory, Jinan University, Guangzhou, China, xjli33@jnu.edu.cn.

¹These authors contribute equally to this work.

Conflict of interest

The authors declare no competing financial interests.

Publisher's Disclaimer: This is a PDF file of an unedited manuscript that has been accepted for publication. As a service to our customers we are providing this early version of the manuscript. The manuscript will undergo copyediting, typesetting, and review of the resulting proof before it is published in its final form. Please note that during the production process errors may be discovered which could affect the content, and all legal disclaimers that apply to the journal pertain.

impaired rotarod and balance beam performance as well as the same sensitivity to seizure induction. Both KI and KO mice show altered formation of SNARE complex and number of synaptic vesicles. In addition, western blotting of KI mouse brain tissues could not detect truncated PRRT2 protein that might be generated by the c.649_650InsC mutation. Moreover, the level of *PRRT2* mRNA in KI mice is significantly decreased, recapitulating the reduction of *PRRT2* mRNA reported in PKD patients. Furthermore, mutant *PRRT2* mRNA is unstable and showed shortened half-life than wild-type *PRRT2* mRNA. Our studies suggest that *PRRT2* frameshift mutation leads to the loss of function by affecting its mRNA stability, a mechanism that is different from haploinsufficiency due to dysfunctional protein or gain of function caused by truncated protein.

Keywords

frameshift mutation; truncated protein; *PRRT2* KI mice; decreased mRNA stability; loss of function

1. Introduction

A heterozygous frameshift *PRRT2* mutation (c.649_650InsC) has been identified as the major causative mutation in *PRRT2* related paroxysmal disorders [1, 2], such as paroxysmal kinesigenic dyskinesia (PKD), benign familial infantile epilepsy, infantile convulsions with choreoathetosis syndrome and paroxysmal hypnogenic dyskinesia [3–8]. However, the clinical symptoms of patients with *PRRT2* mutations show high heterogeneity, and even the same family members carrying identical *PRRT2* mutations exhibit variable symptoms [9], indicating the complex pathogenesis.

PRRT2 is a transmembrane protein with large intracellular N-terminus and short extracellular C terminal dipeptide [10], which suggests that the cytosolic N-terminal region is important for *PRRT2* function. Since PKD is an autosomal dominant disorder and since the common frameshift mutation (c.649_650InsC) may create a truncated *PRRT2* protein that only contains the intracellular N-terminal region [2, 11], although it is postulated that the truncated *PRRT2* leads to a loss of function in PKD [5, 12–14], it remains unknown whether truncated *PRRT2* results in a gain of function *in vivo* and how the mutation causes the loss of function *in vivo*.

Understanding how the frameshift mutation (c.649_650InsC) affects *PRRT2* function is important for developing effective therapeutic strategies for PKD. This is because loss of function can be reversed by restoring the expression of the normal *PRRT2* whereas a gain of function needs to be antagonized by a specific inhibitor. To address this issue, we generated a new *PRRT2* Knock-in (KI) mouse model that expresses human *PRRT2* with the c.649_650InsC mutation to more faithfully mimic the *PRRT2* mutation in PKD patients. We found that this mutation causes a loss of function by affecting the stability of *PRRT2* mRNA. The findings shed new light on the disease mechanism by which mutations in *PRRT2* cause PKD and provide a rationale for treating PKD by restoring the normal level of WT *PRRT2*.

2. Materials and methods

2.1. Animals

To generate a *PRRT2* KO and KI mice, a PGK-Neo 3x stop cassette flanked by loxP sites were inserted into the upstream of endogenous *Prrt2* initiation codon by homologous recombination. Mouse *Prrt2* (from initiation codon to 103 bp in intron 2) was replaced by the corresponding mutant human *PRRT2* cDNA with the c.649_650InsC mutation. At this step, the mouse is a *Prrt2* knockout (KO) model. After KO homozygote mice were crossed with E2a-Cre transgenic mice, PGK-Neo 3x stop cassette was removed and mutant human *PRRT2* is expressed under the endogenous promoter. The heterozygote KI progeny was then crossed with wild type (WT) mice to obtain germline KI mice. Mice were maintained on a 12:12 h light/dark cycle (lights off at 7 p.m.). The temperature was maintained at 22 ± 1 °C with relative humidity (30–70%). All animal procedures were approved by the Institutional Animal Care and Use Committee of Emory University.

2.2. Plasmids and antibodies

Antibodies and plasmids are described in the supplemental materials.

2.3. Mouse behavior tests

Mouse behavior tests were performed as described previously [15, 16]. Detailed procedures are provided in the supplemental materials.

2.4. Flurothyl seizure induction

Seizure induction using flurothyl (2,2,2-trifluoroethyl ether) was performed as previously described [17]. More information is provided in the supplemental materials.

2.5. Cell culture and transfection

Detailed procedures are described in the supplemental materials.

2.6. Western blot

Detailed procedures are described in the supplemental materials.

2.7. Electron microscope

The sections were processed as previously described [18]. See more information in the supplemental materials.

2.8. Stereotaxic injection of the UPS or autophagy inhibitors into mouse brain

Stereotaxic surgery was performed as described previously [19]. Detailed procedures are described in the Supplemental Information.

2.9. RNA extraction and quantitative real-time PCR analysis

Detailed procedures are described in the Supplemental Information.

2.10. Actinomycin D treatment

Detailed procedures are described in the Supplemental Information.

2.11. Statistical Analysis

Data were analyzed using the Prism 8 (GraphPad) software. Statistical significance was determined by two-tailed Student's *t* test or one-way ANOVA. *P* value of less than 0.05 was considered statistically significant. All bar graphs indicate the means, and all error bars represent \pm standard error of the mean (SEM).

3. Results

3.1. Generation of PRRT2 KO and KI mice

Previously reported *PRRT2* KO or mutant rodent models [13, 14, 20] show very mild PKD-like phenotypes under spontaneous conditions. In addition, these phenotypes are not identical, which may result from different gene targeting strategies. It has been reported that a humanized mouse model of Huntington's disease shows severe behavioral and neurodegenerative phenotypes [21]. Thus, we generated a humanized mouse KI model by replacing the mouse *Prprt2* gene with the human *PRRT2* gene harboring c.649dupC mutation, that presumably leads to a truncated *PRRT2* (p.P217fsX7), which should faithfully mimic the mutation in PKD patients (Fig. 1A). Without removing loxP sites by Cre, the targeted mouse is a *Prprt2* null (KO) model. When crossing with Cre, the resulting progeny is KI model. The genotype of KO and KI was confirmed by PCR and DNA sequencing (Fig. 1B and C; and supplementary Fig. 1). Although western blot confirmed the deletion of *PRRT2* protein in KO mice, we could not detect truncated *PRRT2* protein in KI mice using commercial antibody (Fig. 1D), suggesting that its expression may be unstable or is at an undetectable level.

3.2. Comparison of PRRT2 KO and KI mice for their general behavior phenotypes

The *PRRT2* KI model expressing human mutant *PRRT2* under the endogenous promoter has the same genetic background as the *PRRT2* KO mice, providing an ideal model to test whether truncated *PRRT2* will produce PKD-like phenotypes. Generally, both KO and KI mice were born in Mendelian ratio and were indistinguishable from WT littermates in gross appearance. The body weight of KI, KO and WT mice were comparable from 2 to 8 weeks (Fig. 2A). Since PKD is characterized by recurrent, brief attacks of abnormal involuntary movements and the attacks of abnormal movements usually have onset during childhood or adolescence [3, 20, 21], we further examined the motor behavior of homozygous (homo) KO and homo KI mice at 4 and 8 weeks of age, which is equivalent to human adolescence and adulthood respectively. Both KO and KI mice showed decreased duration on rotarod and increased time to cross balance beam (Fig. 2C) at 4 weeks of age, but not at 8 weeks of age, indicating an impaired motor performance at the younger age. There were no other phenotypic differences in elevated plus maze, grip strength, and foot-printing assay at different ages (Fig. 2B–D). Since it was reported that seizure could induce dyskinesia in *PRRT2* mouse models [13, 14], we used flurothyl, an inhaled GABAA receptor antagonist, to induce seizure in mice [17]. We found that both KO and KI mice show shortened latency

in myoclonic jerks, but not in Generalized tonic-clonic seizure stage (Fig. 2E). These results indicated that our *PRRT2* KI model could reproduce the motor defect seen in patients or *Prrt2* KO mouse models [13, 14]. However, KO and KI mice showed no behavioral differences.

3.3. Comparison of PRRT2 KO and KI mice for their synaptic related phenotypes

Since PRRT2 was reported to interact with SNARE complex and is involved in the regulation of synaptic vesicle fusion and neurotransmitter release [14, 20, 24, 25], it is important to know whether truncated PRRT2 would affect the expression of synaptic proteins or the formation of SNARE complex in the mouse brain. Immunoblotting analysis of the whole brain lysates from WT, homo KO and homo KI mice revealed no significant difference at the protein levels of synaptic proteins (Fig. 3A). Western blotting of synaptic proteins in the cerebellum and cortex in heterozygous KI found that, regardless of the reduced expression or absence of PRRT2, the expression of the synaptic proteins was not altered (supplementary Fig. 2), excluding the possibility that truncated PRRT2 exerts dominant negative effect on WT PRRT2 or synaptic proteins.

Next, we examined the influence of truncated PRRT2 on the formation of SNARE complex. It is known that SNARE complex is resistant to the dissociation by SDS at 30°C but completely dissociated when boiled. This property can be used to monitor its complex and monomer status [14, 22]. Full gel western blotting of non-boiled synaptosomes isolated from the whole WT, KO and KI mice brain suggested that the formation of SNARE complex is increased in homo KO and homo KI mice, while the monomer is decreased in KO and KI mice. However, this phenomenon disappeared in Het KO and Het KI mice (Fig. 3B). In addition, electron microscopy (EM) identified a significantly increased number of total synaptic vesicles and docked synaptic vesicles in the nerve terminals from homo KO and homo KI mice compared with WT mice (Fig. 3C and D). These results suggested that absence of PRRT2 did not affect the expression of synaptic proteins, but altered the formation of SNARE complex and increased the number of synaptic vesicles, indicating that PRRT2 may be involved in the synaptic vesicles formation and docking.

3.4. Reduced mRNA stability of mutant PRRT2 leads to undetectable PRRT2 protein

The c.649_650InsC mutation is presumed to generate a truncated PRRT2 protein and our KI mouse model allows to test this possibility. It remains unknown whether commercial antibodies could recognize truncated PRRT2 protein, we therefore developed an N-terminal antibody (EM516), which could react with both WT and truncated PRRT2 protein, to compare the protein levels of WT and mutant PRRT2 (Fig. 4A; supplementary Fig. 3A). It was also confirmed by an antibody to the epitope HA, which is in frame fused to the C-terminal PRRT2. However, the truncated PRRT2 protein is expressed at a markedly lower level than WT PRRT2 (less than 10% of WT) in transfected cells (Fig. 4A and B), which is consistent with the undetectable PRRT2 in the homo KI mouse brain (Fig. 1D). This data suggested that the truncated PRRT2 is either unstable or is inefficiently expressed.

To examine whether truncated PRRT2 is rapidly degraded at the protein level, we injected MG132, a ubiquitin-proteasome system inhibitor or 3-MA, an autophagy-lysosomal system

inhibitor, into the cerebellum of adult homo KI mice using stereotaxic injection. After injection for 12–48 hours, western blotting of the injected brains lysates did not show any truncated PRRT2 protein (Fig. 4C and D), while mHTT that served as positive control could be significantly increased by injection of MG132 and 3-MA (supplementary Fig. 3B). To test whether the reduced level of PRRT2 protein resulted from dysregulated transcription of *PRRT2*, we used quantitative real-time PCR (qPCR) to examine the *PRRT2* mRNA level in the KI mice. The qPCR results showed that the truncated PRRT2 mRNA was significantly decreased in both the cerebellum and cortex of the KI mice compared to mRNA from WT littermates (about 10% of WT *Prrt2* mRNA) (Fig. 4E). To confirm if mutant *PRRT2* mRNA is unstable, we measured the half-life of *PRRT2* mRNA in transfected cells. Actinomycin D (Act D) is a drug that could inhibit cellular transcription and is widely used in measuring the half-life of mRNA [23]. After Act D treatment of HEK 293 cells that expressed WT and mutant PRRT2 respectively, half-life of *PRRT2* mRNA was examined at different time points. The results showed that mutant *PRRT2* mRNA had a significantly shortened half-life than WT PRRT2 mRNA (Fig. 4F–G). Our results suggest that the c.649_650InsC mutation can reduce *PRRT2* mRNA stability, resulting significant low level of mRNA, which in turn produced undetectable PRRT2 protein.

4. Discussion

Previous reports suggest that truncated PRRT2 leads to loss of function [5, 13, 14, 24], however, whether truncated PRRT2 protein is present *in vivo* and whether truncated PRRT2 produces a toxic gain of function remain unclear.

In this study, we generated a new *PRRT2* KI mouse model that faithfully mimics the *PRRT2* frameshift mutation (c.649_650InsC) in PKD patients. The truncated PRRT2 protein is undetectable in our KI mice, which is unlikely due to its rapid degradation, as inhibiting the proteasomal and autophagy degradation via MG132 and 3-MA was unable to increase the level of truncated PRRT2 to allow its detection. On the other hand, our KI model showed dramatically reduced level of mutant *PRRT2* mRNA. This finding explains the loss of function caused by the *PRRT2* mutation and is also consistent with the reduction of *PRRT2* mRNA seen in the PKD patients [12]. In vitro transfection for mRNA half-life study indicated that the mutant *PRRT2* had a significantly reduced mRNA half-life compared to the WT *PRRT2*. Our study provides a new mechanism for the pathogenesis of PKD, which is that the *PRRT2* frameshift mutation decreases its mRNA stability and leads to significant low level of mRNA. As a result, PRRT2 protein is undetectable, resulting in a loss of function in the PKD.

Although how the frameshift mutation affects the stability of *PRRT2* mRNA remains to be investigated, some possibilities may account for this event and need to be tested in the future studies. One possibility is that the mutation creates a new conformation or structure in *PRRT2* RNA, making it prone to degradation. Our results from transfected cells treated with Act D to inhibit cellular transcription suggested that the truncated *PRRT2* mRNA is unstable and can be rapidly degraded. However, these results were obtained from cultured cells, and whether the *PRRT2* frameshift mutation reduces the stability of *PRRT2* mRNA or affects its transcription *in vivo* remains to be investigated.

In addition, by comparing the phenotypes of *PRRT2* KI mice with *Prrt2* KO mice, we found that both KI and KO mice show the same extents of impaired rotarod and balance beam performance as well as the same sensitivity to seizure induction. Interestingly, adolescent *PRRT2* mutant but not adult mutant mice showed PKD-like behavior phenotypes. These phenotypes fit with the phenomenon that the symptoms of patients with *PRRT2* mutations often occur during puberty [3, 22]. Furthermore, increased formation of SNARE complex and increased number of synaptic vesicles near presynaptic membrane were found in both KI and KO mice, suggesting that *PRRT2* may negatively regulate the assemble of SNARE complex and affect the formation and docking of synaptic vesicles. These *in vivo* comparisons demonstrated that the truncated *PRRT2* did not exert dominant negative effect.

In conclusion, we generated a new *PRRT2* KI mouse model that contains the frameshift mutation in PKD patients. Our findings suggest that the frameshift mutation (c. 649_650InsC) leads to the loss of function by affecting its mRNA level, a mechanism that is different from a gain of function mediated by a truncated protein or haploinsufficiency due to dysfunctional protein. Therefore, future development of effective therapeutics of PKD with this mutation in *PRRT2* may need to focus on restoring *PRRT2* mRNA expression rather than blocking the toxic effects of truncated *PRRT2* protein.

Supplementary Material

Refer to Web version on PubMed Central for supplementary material.

Acknowledgements

This work was supported by the National Natural Science Foundation of China (81130021, 81701281, 81501182) and the National Institutes of Health (grant NS036232).

References

- [1]. Li J, Mao X, Wang J, et al., [PRRT2 gene-related paroxysmal disorders], *Zhonghua yi xue yi chuan xue za zhi = Zhonghua yixue yichuanxue zazhi = Chinese journal of medical genetics*. 31 (2014) 595–599. 10.3760/cma.j.issn.1003-9406.2014.01.012. [PubMed: 25297589]
- [2]. Ebrahimi-Fakhari D, Saffari A, Westenberger A, et al., The evolving spectrum of PRRT2-associated paroxysmal diseases, *Brain*. 138 (2015) 3476–3495. 10.1093/brain/awv317. [PubMed: 26598493]
- [3]. Chen WJ, Lin Y, Xiong ZQ, et al., Exome sequencing identifies truncating mutations in PRRT2 that cause paroxysmal kinesigenic dyskinesia, *Nat Genet*. 43 (2011) 1252–1255. 10.1038/ng.1008. [PubMed: 22101681]
- [4]. Wang JL, Cao L, Li XH, et al., Identification of PRRT2 as the causative gene of paroxysmal kinesigenic dyskinesias, *Brain*. 134 (2011) 3493–3501. 10.1093/brain/awr289. [PubMed: 22120146]
- [5]. Lee HY, Huang Y, Bruneau N, et al., Mutations in the gene PRRT2 cause paroxysmal kinesigenic dyskinesia with infantile convulsions, *Cell reports*. 1 (2012) 2–12. 10.1016/j.celrep.2011.11.001. [PubMed: 22832103]
- [6]. Ono S, Yoshiura K, Kinoshita A, et al., Mutations in PRRT2 responsible for paroxysmal kinesigenic dyskinesias also cause benign familial infantile convulsions, *Journal of human genetics*. 57 (2012) 338–341. 10.1038/jhg.2012.23. [PubMed: 22399141]
- [7]. Wang JL, Mao X, Hu ZM, et al., Mutation analysis of PRRT2 in two Chinese BFIS families and nomenclature of PRRT2 related paroxysmal diseases, *Neurosci Lett*. 552 (2013) 40–45. 10.1016/j.neulet.2013.07.020. [PubMed: 23896529]

- [8]. Liu XR, Huang D, Wang J, et al., Paroxysmal hypnogenic dyskinesia is associated with mutations in the PRRT2 gene, *Neurol Genet.* 2 (2016) e66 10.1212/NXG.0000000000000066. [PubMed: 27123484]
- [9]. Brueckner F, Kohl B, Puest B, et al., Unusual variability of PRRT2 linked phenotypes within a family, *Eur J Paediatr Neurol.* 18 (2014) 540–542. 10.1016/j.ejpn.2014.03.012. [PubMed: 24755245]
- [10]. Rossi P, Sterlini B, Castroflorio E, et al., Novel Topology of Proline-Rich Transmembrane Protein 2 (PRRT2): Hints for an Intracellular Function at the Synapse, *J Biol Chem.* (2016). 10.1074/jbc.M115.683888.
- [11]. Valtorta F, Benfenati F, Zara F, et al., PRRT2: from Paroxysmal Disorders to Regulation of Synaptic Function, *Trends Neurosci.* 39 (2016) 668–679. 10.1016/j.tins.2016.08.005. [PubMed: 27624551]
- [12]. Wu L, Tang HD, Huang XJ, et al., PRRT2 truncated mutations lead to nonsense-mediated mRNA decay in Paroxysmal Kinesigenic Dyskinesia, Parkinsonism & related disorders. 20 (2014) 1399–1404. 10.1016/j.parkreldis.2014.10.012. [PubMed: 25457817]
- [13]. Michetti C, Castroflorio E, Marchionni I, et al., The PRRT2 knockout mouse recapitulates the neurological diseases associated with PRRT2 mutations, *Neurobiol Dis.* 99 (2017) 66–83. <https://doi.org/10.1016/j.nbd.2016.12.018>. [PubMed: 28007585]
- [14]. Tan GH, Liu YY, Wang L, et al., PRRT2 deficiency induces paroxysmal kinesigenic dyskinesia by regulating synaptic transmission in cerebellum, *Cell research.* 28 (2018) 90–110. 10.1038/cr.2017.128. [PubMed: 29056747]
- [15]. Yang S, Chang R, Yang H, et al., CRISPR/Cas9-mediated gene editing ameliorates neurotoxicity in mouse model of Huntington's disease, *J Clin Invest.* 127 (2017) 2719–2724. 10.1172/JCI92087. [PubMed: 28628038]
- [16]. Yang Y, Yang S, Guo J, et al., Synergistic Toxicity of Polyglutamine-Expanded TATA-Binding Protein in Glia and Neuronal Cells: Therapeutic Implications for Spinocerebellar Ataxia 17, *J Neurosci.* 37 (2017) 9101–9115. 10.1523/JNEUROSCI.0111-17.2017. [PubMed: 28821675]
- [17]. Makinson CD, Tanaka BS, Lamar T, et al., Role of the hippocampus in Nav1.6 (Scn8a) mediated seizure resistance, *Neurobiol Dis.* 68 (2014) 16–25. 10.1016/j.nbd.2014.03.014. [PubMed: 24704313]
- [18]. Huang B, Wei W, Wang G, et al., Mutant huntingtin downregulates myelin regulatory factor-mediated myelin gene expression and affects mature oligodendrocytes, *Neuron.* 85 (2015) 1212–1226. 10.1016/j.neuron.2015.02.026. [PubMed: 25789755]
- [19]. Li X, Wang CE, Huang S, et al., Inhibiting the ubiquitin-proteasome system leads to preferential accumulation of toxic N-terminal mutant huntingtin fragments, *Hum Mol Genet.* 19 (2010) 2445–2455. 10.1093/hmg/ddq127. [PubMed: 20354076]
- [20]. Goodenough DJ, Fariello RG, Annis BL, et al., Familial and acquired paroxysmal dyskinesias. A proposed classification with delineation of clinical features, *Archives of neurology.* 35 (1978) 827–831. 10.1001/archneur.1978.00500360051010. [PubMed: 718486]
- [21]. Bruno MK, Hallett M, Gwinn-Hardy K, et al., Clinical evaluation of idiopathic paroxysmal kinesigenic dyskinesia: new diagnostic criteria, *Neurology.* 63 (2004) 2280–2287. 10.1212/01.WNL.0000147298.05983.50. [PubMed: 15623687]
- [22]. Otto H, Hanson PI, Jahn R, Assembly and disassembly of a ternary complex of synaptobrevin, syntaxin, and SNAP-25 in the membrane of synaptic vesicles, *Proc Natl Acad Sci U S A.* 94 (1997) 6197–6201. 10.1073/pnas.94.12.6197. [PubMed: 9177194]
- [23]. Sobell HM, Actinomycin and DNA transcription, *Proc Natl Acad Sci U S A.* 82 (1985) 5328–5331. 10.1073/pnas.82.16.5328. [PubMed: 2410919]
- [24]. Ji Z, Su Q, Hu L, et al., Novel loss-of-function PRRT2 mutation causes paroxysmal kinesigenic dyskinesia in a Han Chinese family, *BMC neurology.* 14 (2014) 146 10.1186/1471-2377-14-146. [PubMed: 25027704]

Highlights

- *PRRT2* KI mice with frameshift mutation do not have detectable truncated *PRRT2* protein.
- KI mice show dramatically reduced level of mutant *PRRT2* mRNA.
- Frameshift mutation reduces *PRRT2* mRNA stability to cause loss of function.
- Both *PRRT2* KI and KO mice show comparable PKD-like behavioral phenotypes.
- The formation of SNARE complex and number of synaptic vesicles are increased in adult *PRRT2* mutant mice.

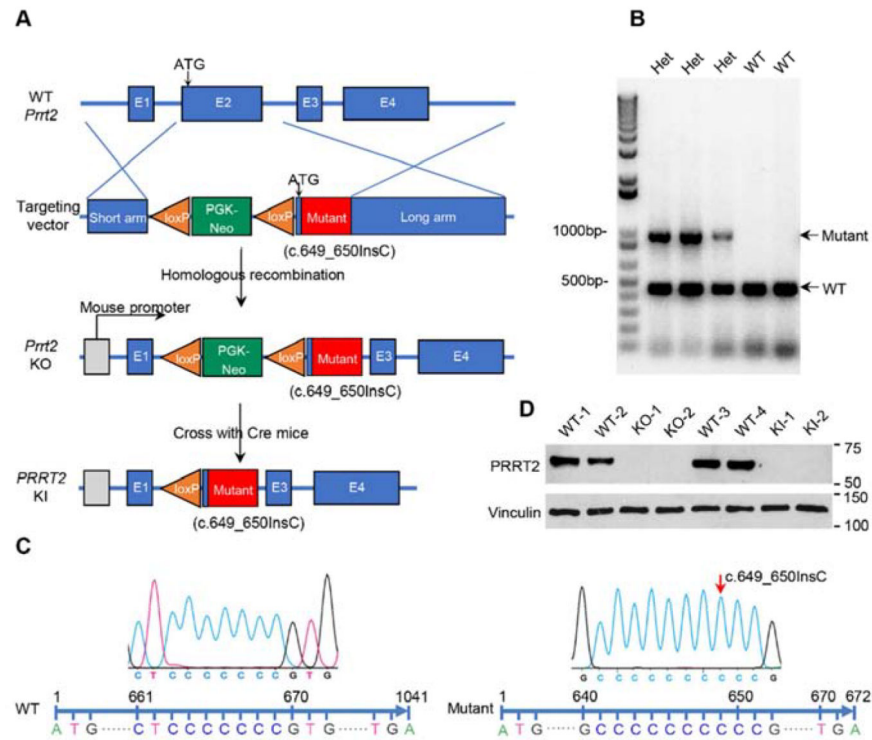


Fig. 1. Generation of *PRRT2* KO and KI mice.

(A) Schematic diagram of generation of mutant *PRRT2* mice. (B) Genotyping of WT and mutant mice using genomic DNA from mouse tail by PCR. (C) Sequencing results of WT and Mutant mice. (D) Western blotting of the cerebellum lysates from WT, KO and KI.

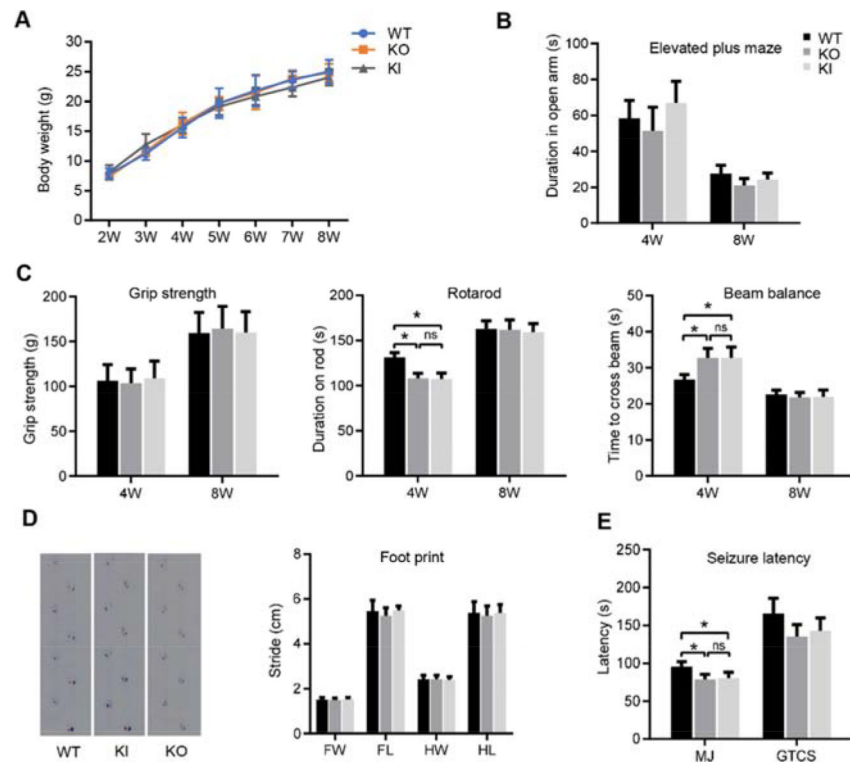


Fig. 2. Comparable PKD-like behavioral phenotypes in *PRRT2* KO and KI mice.

(A) Body weight of WT, KO and KI mice from 2 to 8 weeks of age. (B) Elevated plus maze assay of WT, KO and KI mice at 4 and 8 weeks of age. (C) Motor behavior of WT, KO and KI mice at 4 and 8 weeks of age in grip strength, rotarod and beam balance. (D) Foot-printing assay on WT, KO and KI at the age of 8 weeks. FW, fore-paw width; FL, fore-paw length; HW, hind-paw width; HL, hind-paw length, were recorded. Age-matched WT mice (n=24), KO mice (n=15) and KI mice (n = 15) were examined in above assays. (E) Flurothyl-induce seizure experiments on WT, KO and KI mice at 8 weeks of age. Latency to first myoclonic jerks (MJ) and generalized tonic-clonic seizure (GTCS) were recorded. One-way ANOVA followed with Turkey's multiple comparisons test, * $P < 0.05$, n=10 per group.

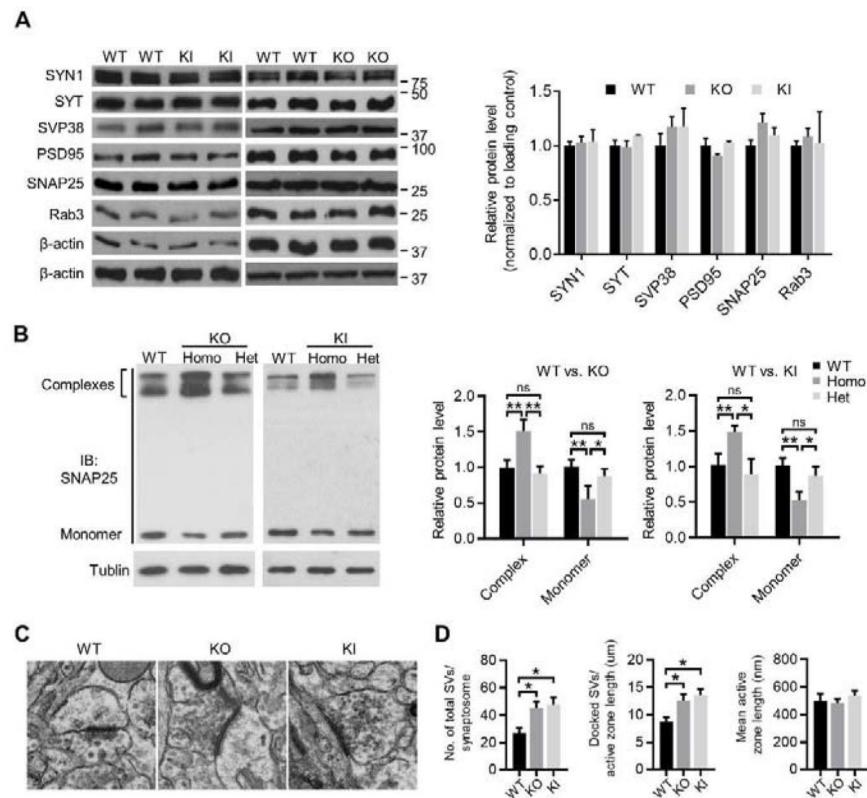


Fig. 3. Increased formation of SNARE complex and number of synaptic vesicles in *PRRT2* KO and KI mice.

(A) Western blotting of adult WT, KO and KI mice brain tissues with synapse related protein. SYN1, Synapsin1; SYT, Synaptotagmin. STX1A, Syntaxin1A. One-way ANNOVA followed with Turkey's multiple comparisons test, $n=6$ per group. (B) Full gel western blotting of non-boiled synaptosomes purified from the whole brain tissues of 2-month-old WT, KO and KI mice. One-way ANNOVA followed with Turkey's multiple comparisons test, $*P < 0.05$, $**P < 0.005$, $n=3$ per group. (C) Representative transmission electron microscopy images of nerve terminals from 2-month-old WT, *PRRT2* KO and KI mice. Scale bar, 100 nm. (D) Quantitative analysis of total synaptic vesicles (SVs), docked SVs and mean length of active zone. One-way ANNOVA followed with Tukey's multiple comparisons test, $*P < 0.05$, $n=3$ per group.

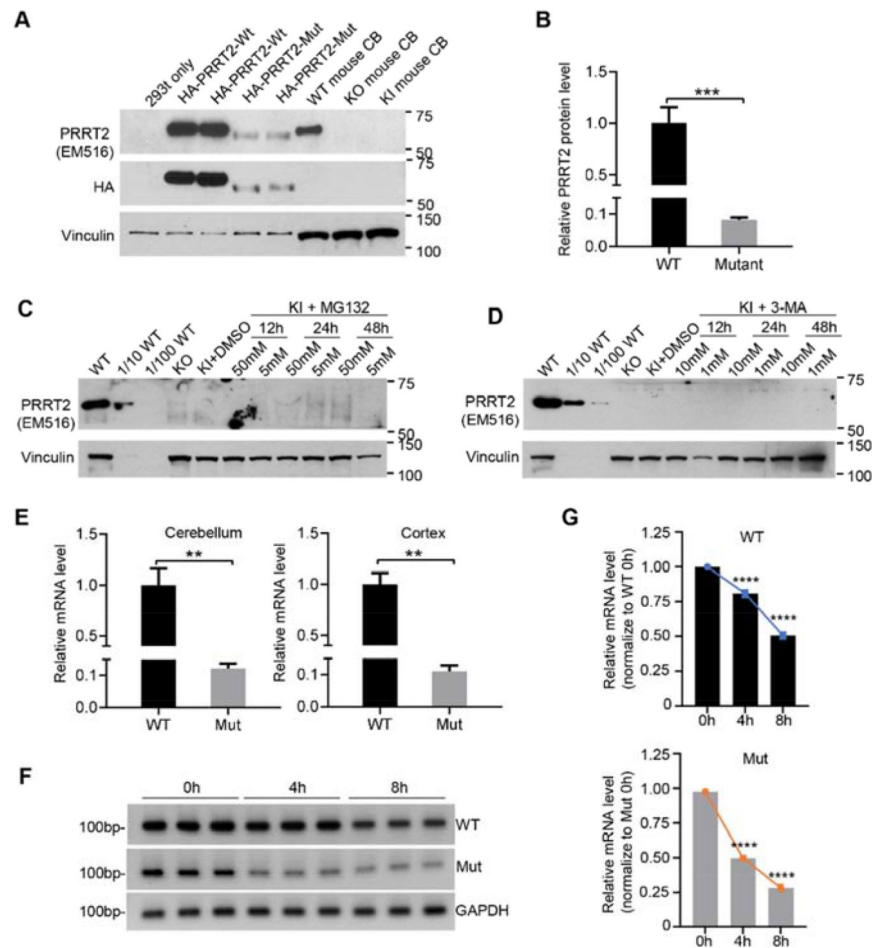


Fig. 4. Reduced mRNA stability of mutant *PRRT2* leads to undetectable *PRRT2* protein. (A-B) Western blotting of transfected HEK293 cells and adult mouse cortex lysates. The blots were probed with anti-*PRRT2* antibody (EM516) and anti-HA antibody. Vinculin served as a loading control. Unpaired-student's t test, *** $P=0.001$, $n=4$ per group. (C-D) Western blotting of WT, KO and KI mice cerebellum injected with MG132 (C) or 3-MA (D) with the indicated concentrations and times. (E) Quantitative real-time PCR (qPCR) assay of WT and mutant *PRRT2* mRNA in the cerebellum and cortex of adult WT and KI. Unpaired-student's t test, $n=4$ per group, ** $P=0.0056$ (cerebellum), ** $P=0.0014$ (cortex). (F-G) QPCR assay on the half-life of WT and mutant *PRRT2* mRNA in transfected Hek293 cells after Actinomycin D treatment at different time point. One-way ANOVA followed with Tukey's multiple comparisons test, **** $P < 0.0001$, $n=6$ per group.